Adjustable Speed Drive Control Based on Random Pulse Width Modulation

Shin Kim, Eric Benedict, Fereshteh Fatehi, Nimish Patel, Abdollah Homaifar, Thomas A. Lipo

Center for Power Electronics Systems
The Department of Electrical Engineering
North Carolina A&T State University
Greensboro, NC 27411 USA
Tel: (336) 334-3151, Fax: (336) 334-7934

***Abstract* – The Pulse Width Modulation (PWM) power electronics systems often produce objectionable acoustic noise at the PWM switching frequency. For example, in a fan / blower drive, the drive used for the blower should use "spread spectrum PWM" technology (also known as Random PWM) where acoustic noise radiating through the duckwork is a very seriously concerned. This paper shows the theoretical basis for the control strategy and simulation results are presented by the random switching conditions. The system consists of a single-phase induction motor by connecting the main and auxiliary winding of the motor across the bridge as an unbalanced three-phase load and the step-up (boost) converter in order to pop-up the DC bus voltage.**

I. INTRODUCTION

Single-phase induction motors are one of the most widely used types of low power motors in the world, especially for domestic or commercial applications where a three-phase power supply is not available. However, speed modulation of a single-phase motor is usually achieved either by non-electrical means, such as throttling the mechanical output from the motor while it continues to run at full speed, or by switching windings to change the number of motor poles for different operating condition as required [1].

Only a few alternatives have been reported as to the use of variable frequency converters to achieve continuous variable speed single-phase motor operation. One of these approaches uses a single-phase converter to control the phase angle of the voltage applied to the motor auxiliary winding, while the main winding remains connected to the ac supply [2]. Other works have reported the performance of a standard motor when driven from a single-phase variable frequency supply [3], [4], using an unmodified capacitor run type motor.

These investigations have shown that a standard single-phase motor has a quite limited performance, and that while controlling the phase angle of the voltage applied to the auxiliary winding can achieve variable speed operation [2].

An alternative solution to the development of a single-phase variable speed drive system would be to rectify the incoming ac supply to create a dc bus voltage and to use a three-phase variable motor supplied from a Variable Voltage Variable Frequency (VVVF) inverter drive system. The only variation compared to a conventional three-phase drive system would be the reduced dc bus voltage that can be obtained from the single-phase ac supply.

Nevertheless, there remains some considerable attraction in the concept of a variable speed single-phase motor drive system for retrofit situations, where a three-phase replacement motor cannot be easily substituted for an existing motor because of mechanical, structural or simply cost constraints. In addition, since a single-phase induction motor is most often an unbalanced two phase motor, any single-phase motor variable speed controller that has developed would almost certainly be able to control the speed of a balanced two phase motor. This would have application in other areas, such as for small frame motors, where a two-phase winding arrangement is sometimes easier to realize physically than a three-phase winding set.

In this paper, an approach is presented for continuous variable speed control of a single-phase induction motor, using a random PWM (RPWM) and step-up chopper. The modulation strategy treats the motor's main and auxiliary windings as a set of unbalanced two-phase windings at 60 Hz. The simulation results of a sinusoidal PWM (SPWM) and RPWM with the same parameters are compared. The results illustrate the reduction of noise by using RPWM scheme.

II. SYSTEM DESCRIPTION

The state of the art for variable speed can best be compared with, what may be considered as the "ideal" converter situation shown in Fig. 1 [5]. In this case, both the input side and output side converters are full transistor bridge, the input side being a single-phase bridge (necessary since the source is assumed to be single-phase) and the output being a three-phase bridge. The machine for the "ideal" case is assumed to be a three-phase squirrel cage induction motor, which guarantees a relatively low cost combined with good efficiency. This converter has a total of 10 transistor switches, clearly an expensive alternative.

This work was supported primarily by the ERC Program of the National Science Foundation under Award Number EEC-9731677.

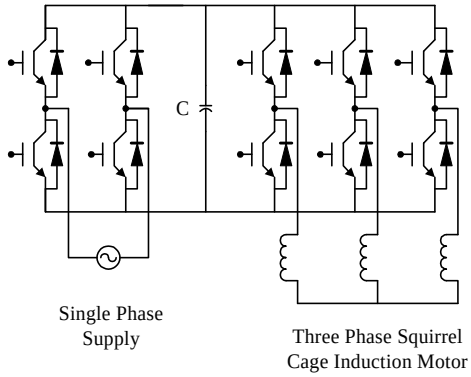

Fig. 1. The Ideal Case Variable Speed Drive

Fig. 2 shows the reduced cost motor drives from York International Company [6], [7], [8].

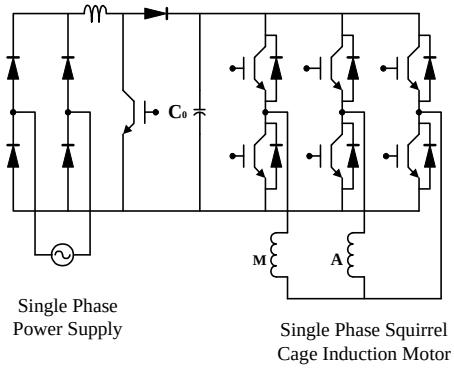

Fig. 2. Voltage Boost Two-Phase Variable Speed Drive

The four switches of the input have been replaced by a diode bridge and a single transistor step-up chopper, reducing the number of switches to 7 transistors. A single-phase motor is used allowing direct connection of the motor to the single-phase supply in the event of a converter failure. The step-up chopper allows pump up of the dc link to a higher voltage than being achieved by a simple diode bridge. This allows the use of a conventional single-phase motor, which requires a larger voltage than the rated voltage to achieve speeds greater than rated speed.

III. PRINCIPLE OPERATION

Most single-phase motors are constructed with two windings which are physically displaced 90 electrical degrees around the motor stator. The windings are often asymmetrical, in which case the "main" winding will have a higher current rating. Furthermore, the "auxiliary" winding is connected to the ac supply through a series capacitor, as shown in Fig. 3, to make its current lead the main winding current by approximately 90° in phase. The time and spatial quadrature currents in the two windings create an unbalanced tow-phase rotating magnetic field which ensures that some motor torque is generated even at standstill.

Single-phase motors operate either as "capacitor-run", where the auxiliary winding is permanently energized, or as "capacitor-start", where the auxiliary winding is switched out of circuit by a centrifugal switch as the motor speeds up. The auxiliary winding of a capacitor-start single-phase motor is generally not rated for continuous operation, but is connected only at low motor speeds to create a motor starting torque.

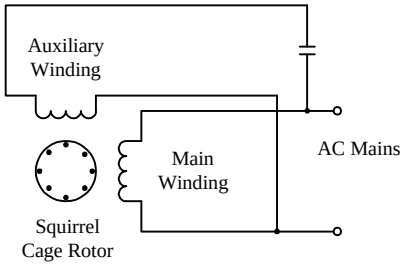

Fig. 3. Capacitor-Run Single Phase Induction Motor

The series capacitor is ideally chosen so that the main and auxiliary winding currents are time displaced by 90°, achieving exact two-phase operation except for the unbalanced current magnitudes. However, this optimum condition only occurs for a particular motor speed, since the effective impedance of both windings vary significantly with motor slip. Conventional single-phase motors sometimes improve this situation by using two series capacitors, in a capacitor-start / capacitor-run configuration, so that exact quadrature time displacement of the currents can occur at least at standstill and at the motor's normal operating speed.

For variable speed control, the voltage applied to the main and auxiliary windings should be of variable frequency, and such magnitude and phase orientation as to maintain the winding currents in time quadrature at all times. One of the approaches to achieve this would be to use PWM bridge so as to create the required fundamental ac voltage.

An alternative approach is to use 6 switches three-phase PWM, connecting the two motor windings as an unbalanced load between two phases, as shown in Fig. 2. This is a more cost effective solution, especially when it is recognized that 6 elements of power electronic switches are now available as a single power electronic module for the power levels of interest (less than a few kW). Note however that the switch rating must be increased by $\sqrt{2}$ compared to the rated motor current, since the center phase carries the sum of the both winding currents which is not zero (unlike a three-phase winding neutral connection). In practice, this will not be a significant limitation for low power motor, given the ratings of present day power electronic switches.

In order to control a single-phase motor with such a converter configuration, it is necessary to determine how the

motor will respond to a variable supply frequency across both windings, and determine modulation strategy that most effectively achieve the objective of maintaining quadrature winding *currents* at any fundamental frequency. Alternatively, for a simple controller, it will probably be easier to modulate for quadrature *voltages* across the windings, correcting for any difference between the winding impedance angles.

IV. UNSYMMETRICAL TWO-WINDING INDUCTION MACHINE

For the purposes of analysis, we can consider the unsymmetrical two-phase induction machine. The analysis of such machines can be conveniently handled by the normal *d-q* model approach used for three-phase machines. The detail of the derivation of the *d-q* model as applied to unsymmetrical two-phase induction machines are described in [9]. The equivalent circuit of unsymmetrical two-phase induction machine is shown in Fig. 4.

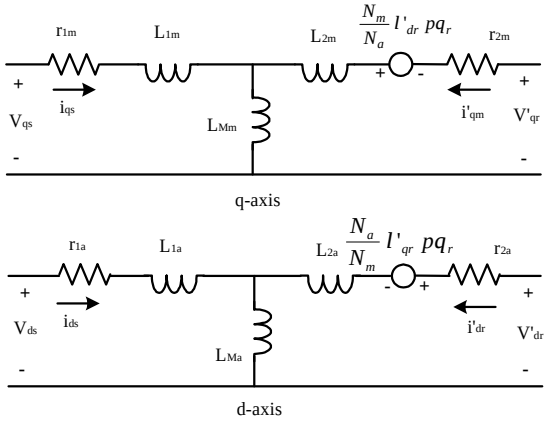

Fig. 4. Equivalent Circuits (*d* and *q*) of Unsymmetrical Two-phase Induction Machine

In order to simulate unsymmetrical two-phase induction machine, the simulation model is constructed by normalized flux model. For transient analysis the governing equations consist of

1. 5 coupled non-linear differential equations: These include 4 linear differential equations with constant speed and the torque equation.
2. Slow mechanical transient: the steady-state vs. rotor speed (w_r) which yield non-linear equation (torque equation).
3. Constant speed: 4 linear differential equations with time varying coefficients.

The zero sequence quantities are neglected for simplicity and the governing equations are given below.

$$i_{qs} = \frac{1}{X_{1m}}\left(y_{qs} - y_{Mq}\right) \tag{1}$$

$$i_{ds} = \frac{1}{X_{1a}}\left(y_{ds} - y_{Md}\right) \tag{2}$$

$$i'_{qr} = \frac{1}{X_{2m}}\left(y'_{qr} - y_{Mq}\right) \tag{3}$$

$$i'_{dr} = \frac{1}{X_{2a}}\left(y'_{dr} - y_{Md}\right) \tag{4}$$

where

$$y_{Mq} = X_{Mm}\left(i_{qs} - i'_{qr}\right) \tag{5}$$

$$y_{Md} = X_{Ma}\left(i_{ds} - i'_{dr}\right) \tag{6}$$

In these equations,

$$y_{qs} = w_e l_{qs} \tag{7}$$

where w_e is the base electrical angular velocity corresponding to rated frequency.

If Equ. (1) through (4) are substituted for the currents in Equ. (5) and (6), then the equations are obtained as y_{qs}, y_{ds}, y'_{qr}, y'_{dr}:

$$y_{qs} = \frac{w_e}{p}\left[v_{qs} + \frac{r_{1m}}{X_{1m}}\left(y_{Mq} - y_{qs}\right)\right] \tag{8}$$

$$y_{ds} = \frac{w_e}{p}\left[v_{ds} + \frac{r_{1a}}{X_{1a}}\left(y_{Md} - y_{ds}\right)\right] \tag{9}$$

$$y'_{qr} = \frac{w_e}{p}\left[v'_{qr} + \frac{N_m}{N_a}\cdot\frac{w_r}{w_e}\cdot y'_{dr} + \frac{r_{2m}}{X_{2m}}\left(y_{Mq} - y'_{qr}\right)\right] \tag{10}$$

$$y'_{dr} = \frac{w_e}{p}\left[v'_{dr} - \frac{N_a}{N_m}\cdot\frac{w_r}{w_e}\cdot y'_{qr} + \frac{r_{2a}}{X_{2a}}\left(y_{Md} - y'_{dr}\right)\right] \tag{11}$$

where, $p = \frac{d}{dt}$, and

$$y_{Mq} = X_{qm}\left(\frac{y_{qs}}{X_{1m}} + \frac{y'_{qr}}{X_{2m}}\right) \tag{12}$$

$$y_{Md} = X_{da}\left(\frac{y_{ds}}{X_{1a}} + \frac{y'_{dr}}{X_{2a}}\right) \tag{13}$$

in which

$$X_{qm} = \frac{1}{\left(\frac{1}{X_{Mm}}\right) + \left(\frac{1}{X_{1m}}\right) + \left(\frac{1}{X_{2m}}\right)} \tag{14}$$

$$X_{da} = \frac{1}{\left(\frac{1}{X_{Ma}}\right)+\left(\frac{1}{X_{1a}}\right)+\left(\frac{1}{X_{2a}}\right)} \quad (15)$$

In these equations, w_r is the rotor speed in electrical radians per second.

Although the currents can also be eliminated from torque expression, it is generally desirable to observe the four currents. Therefore, it is convenient to obtain the instantaneous torque by using

$$T = \frac{P}{2}\frac{1}{w_e}\left(\frac{N_a}{N_m}y'_{qr}i'_{dr} - \frac{N_m}{N_a}y'_{dr}i'_{qr}\right) \quad (16)$$

where, P is the number of pole of the machines.

V. RANDOM PULSE WIDTH MODULATION (RPWM)

This method has been recently used to minimize PWM mechanical vibration in the motor drives [10]. Reference [10] shows that if either the pulse position or the switching frequency is varied in a random manner, the power spectrum of the output voltage of the converter acquires a continuous part, while the discrete (harmonics) part is significantly reduced. There are three basic concepts that are utilized in the existing RPWM strategies, which are briefly descried as follows [11].

A. Randomized Switching Frequency

Randomization of the switching frequency has been the most common means of RPWM. It can be performed in either regular or natural sampling mode. The regular sampling mode, employed in inverters, is characterized by an integer number, N, of switching intervals per cycle of the output frequency. N can be randomly changed from cycle to cycle.

The natural sampling method is obtained using either the classic triangulation or the PWM space vector method. In triangulation method, the triangular carrier signal, with which the reference voltage signal is compared, is generated with a randomly varying slope. Fig. 5 shows a triangular carrier signal that uses this method of randomization.

B. Randomized Pulse Position

In the randomized pulse position, the pulses of switching signals are randomly placed in individual switching intervals. The simplest approach consists of random selection of only two possible positions, which is called lead-lag RPWM. Fig. 6 is an example of these switching pulses.

C. Random Switching

In the random switching method, randomly fractional numbers, r, having uniform probability distribution, are compared with the desired duty cycle of the switching signals for individual phases of the inverter.

However, the method has a significant drawback, which is the rapid deterioration of quality of operation at low values of modulation [10].

In this study we have chosen the natural sampling method.

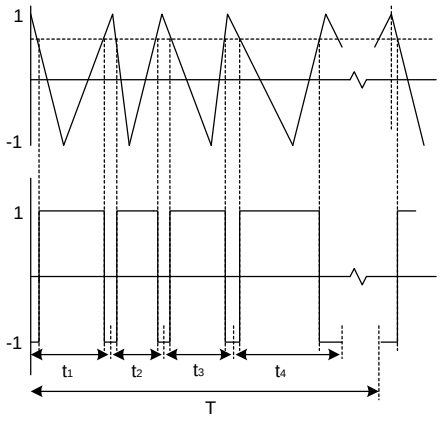

Fig. 5. The Randomized Triangular Method for Generating RPWM

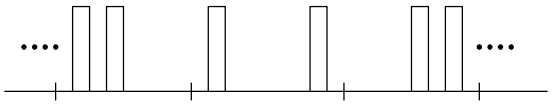

Fig. 6. Some of Modulator Pulses in the lead-lag RPWM Techniques

VI. CONVERTER MODULATION STARTEGY

In this section, two different modulation strategies for the sinusoidal PWM of a three-leg inverter are introduced [12]. The first strategy is to hold the common terminal at the mid-point of the DC bus and then modulate the two remaining phases to achieve the following voltage set of:

$$V_a = |V_{main}|\cos(wt) + \frac{V_{dc}}{2} \quad (17)$$

$$V_b = |V_{aux}|\sin(wt) + \frac{V_{dc}}{2} \quad (18)$$

$$V_c = \frac{V_{dc}}{2} \quad (19)$$

where, V_a, V_b, V_c is the inverter phase voltage, w is the angular frequency, and V_{dc} is the DC bus voltage. The vector diagram showing this modulation scheme is shown in Fig. 7. The dotted circle represents the maximum output voltage which a single inverter leg is capable of producing. The per unit base, 1.0 pu, corresponds to the DC Bus voltage. From

this figure, it is clear that for this modulation strategy, the peak obtainable voltage from a 1.0 pu DC bus is limited to 0.5 pu.

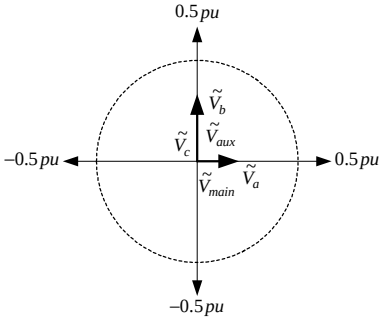

Figure 7. Simple Modulation Voltage Phasor Diagram

The second modulation strategy is similar to the third harmonic injection technique [13]. In this improved strategy, they inject a fixed common mode AC signal into each of three-phase leg voltages to increase the peak obtainable voltage. The three-phase leg voltages become:

$$V_a = |V_{main}| \cos(wt) + 0.5\cos(wt + d) + \frac{V_{dc}}{2} \quad (20)$$

$$V_b = |V_{aux}| \sin(wt) + 0.5\cos(wt + d) + \frac{V_{dc}}{2} \quad (21)$$

$$V_c = 0.5\cos(wt + d) + \frac{V_{dc}}{2} \quad (22)$$

where

$$d = \tan^{-1}\left(-\frac{V_{aux}^{\max}}{V_{main}^{\max}}\right) \quad (23)$$

which gives rise to following modulation limitations:

1. The maximum possible peak voltage while the winding voltages remains in quadrature occurs at δ = -135°, and has a magnitude of :

$$V_{main}^{\max} = V_{aux}^{\max} = \frac{1}{\sqrt{2}}\, pu \quad (24)$$

2. Some trade-offs between the magnitudes of the two-phase voltages can be considered if the quadrature constraint its relaxed, or a non-unity ratio between the two voltages is desired. For example, if $V_{aux}^{\max}$ =0, $V_{main}^{\max}$ can increase to 1 pu as δ goes to zero, i.e. a maximum voltage transfer ratio of 1.0. Under these conditions, phase legs "a" and "c" act as a single-phase bridge, and the voltage across the auxiliary winding reduces to zero. Alternatively, if the winding voltages cease to be in quadrature, and instead are moved together into phase, the maximum possible peak voltages can increase to 1.0 pu, with δ becoming zero. Under this condition, phase legs "a" and "b" become identical.

The phasor diagram for this modulation scheme is shown in Fig. 8. Note that the phasor voltages $\tilde{V}_a$, $\tilde{V}_b$, $\tilde{V}_c$ are not equal in magnitude.

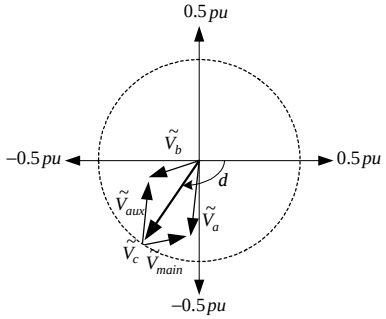

Figure 8. Common-Mode Injection Modulation Voltage Phasor Diagram

VII. PROPOSED MODULATION STRATEGY

The control algorithm, which has been implemented, is adapted from [14]. It uses a three-phase inverter to generate a two-phase voltage with the required 90° phase shift between the two phases, and an arbitrary amplitude ratio of the two vectors. This method is used to compensate for the increased impedance of the auxiliary winding in the single-phase motor. The method is discussed next. An important property of this modulation scheme is that all three generated phase voltages, V_a, V_b, and V_c have the same amplitude.

$$|V_a| = |V_b| = |V_c| \quad (25)$$

This will make the voltage stress on all devices equal, improve the device utilization and provide the maximum possible output voltage for a given DC bus voltage. This constraint is incorporated in the phasor diagram Fig. 9, since each phasor has a length equal to V_1. Observation of the figure shows that the main and auxiliary winding voltages are simply

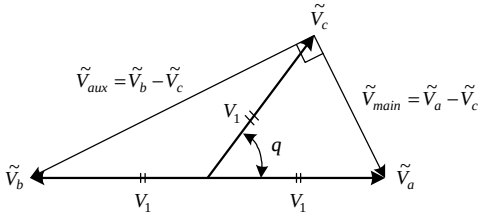

Figure 9. Voltage Phase Diagram

$$\tilde{V}_{aux} = \tilde{V}_b - \tilde{V}_c \qquad \tilde{V}_{main} = \tilde{V}_a - \tilde{V}_c \tag{26}$$

and that the ratio between the main winding voltage and the auxiliary winding voltage is the same as turn ratio.

$$\tilde{V}_{aux} = \frac{N_a}{N_m} \cdot \tilde{V}_{main} \tag{27}$$

Performing basic trigonometry, q can be found to be

$$q = 180^\circ - 2 \cdot \tan^{-1}(a) \tag{28}$$

where,

$$a = \frac{\tilde{V}_{aux}}{\tilde{V}_{main}} \tag{29}$$

and that V_1 is obtained by applying the Pythagorean theorem.

$$V_1 = \tilde{V}_{main} \cdot \frac{\sqrt{1+a^2}}{2} \tag{30}$$

The phasor diagram for the proposed modulation scheme in a format similar to the common-mode injection modulation voltage scheme of Fig. 8 is shown in Fig. 10.

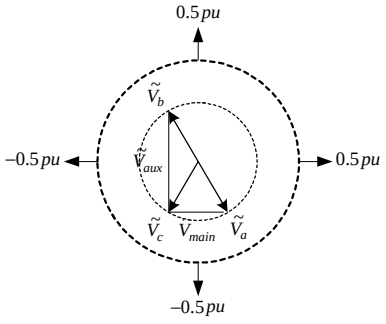

Figure 10. Proposed Modulation Scheme Voltage Phasor Diagram

VIII. SIMULATION RESULTS

Theoretical computations of the adjustable speed drive (ASD) system have been simulated by MATLAB/SIMULINK software. The machine simulation parameters are based on the ¾ HP experimental machine described in Table 1.

TABLE 1: ¾ HP, 6 pole, 230V, 60Hz Motor Parameters

r1m	8.69 Ω	r2m	9.91 Ω
L1m	0.0328 H	L2m	0.0328 H
r1a	21.8 Ω	r2a	20.8 Ω
L1a	0.0607 H	L2a	0.0607 H
L_{Mm}	0.366 H	L_{Ma}	0.366 H

Fig. 11 illustrates the PWM output voltage. In this figure, the V_{main} and V_{aux} should be 90° phase shifted. Also, the V_{aux} should be greater than V_{main} where its peak value is around 530 V. In order to observe the 90° phase shift/amplitude difference, the fundamental components of PWM output are plotted in Fig. 12. These figures clearly show those differences.

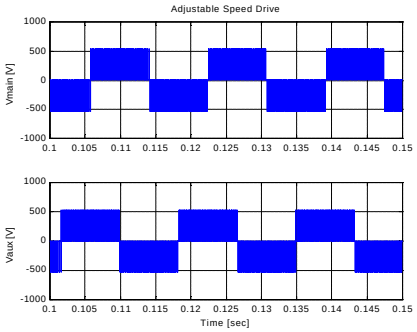

Figure 11. The PWM Inverter Output Voltages

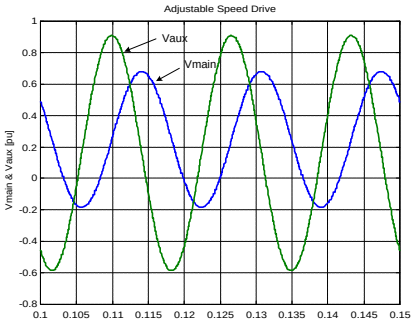

Figure 12. The Fundamental Component of PWM Inverter Output Inverter output Voltage

Fig. 13 shows the single-phase induction motor rotor speed and its torque characteristics. The rotor speed approached 1.0 pu since motor frequency is 60 Hz.

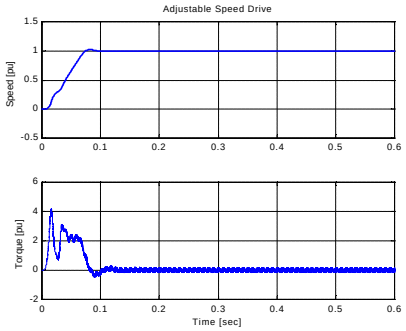

Figure 13. Single-Phase Induction Motor Characteristics – Speed & Torque

Fig. 14 shows the speed and torque characteristics as the speed changes from full speed (60 Hz) to half speed (30 Hz) after 0.4 sec.

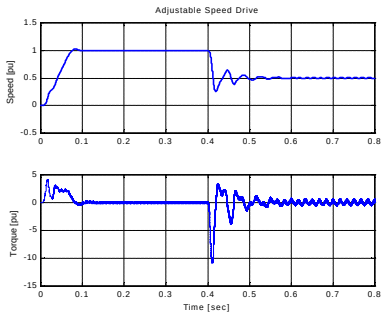

Figure 14. Changing Frequency from 60 Hz to 30 Hz and its characteristics

Fig. 15 shows the motor output current, i_{main} and i_{aux}. In contrast to V_{main} and V_{aux}, the i_{main} is greater than the i_{aux} , which depends on turn ratio. The relationship between motor output currents is given in Equ. (35).

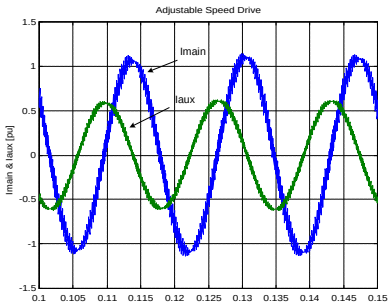

$_{main}$ & i_{aux}

Fig. 16 shows the motor winding current as a trajectory and when α is factored into the current, the scaled current trajectory represents the stator MMF trajectory.

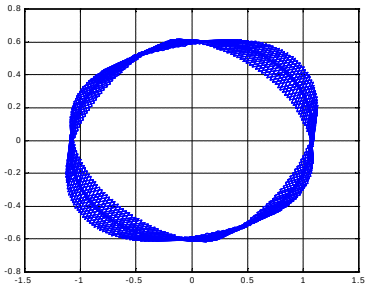

Figure 16. The Motor Current and Stator MMF Trajectory

Examination of the current trajectory ellipse shows that the major axis of the ellipse is not perfectly horizontal which is expected since the simplified case is being simulated. This resulted in the MMF trajectory being a distorted circle.

The converter operation both with SPWM and RPWM control units and noise equivalent circuit has been simulated. The simulation results are shown in Fig. 17. and Fig. 18.

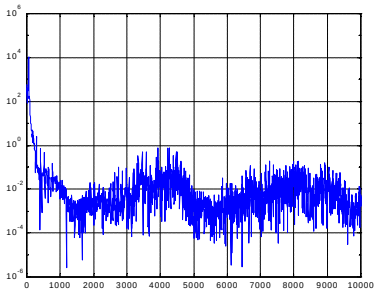

Figure 17. Frequency Spectrum Analysis using SPWM

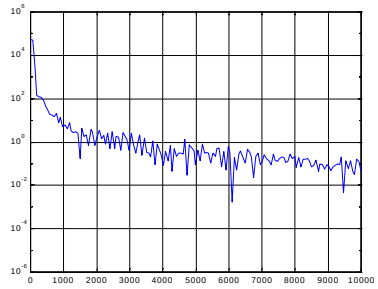

Figure 18. Frequency Spectrum Analysis using RPWM

Fig. 17 shows the current frequency spectrum using SPWM and Fig. 18 the current frequency spectrum using RPWM. Those converters use PWM technique for current shaping and the switching frequency is set at 5kHz. It is clear that the frequency harmonics using SPWM have been more concentrated rather than using RPWM. Therefore, Using RPWM scheme is much better than using SPWM scheme in order to reduce the acoustic noise factor.

VIII. CONCLUSION

This paper proposes a method for modulating a PWM scheme to achieve variable speed operation of an unbalanced two winding induction motor. It investigates the motor operation and shows the characteristics. From these investigations, a precise modulation strategy is proposed for the variable frequency, so that this system can be achieve from the motor at any speed with the motor operating at a small slip.

Also, an alternative method namely RPWM to shape the input current of this type of converter was proposed. Through simulation, it has been shown that due to spreading effect of the RPWM in frequency domain, this technique is an

effective way to reduce EMI noise emanating from the converter. The strategy has been verified in MATLAB / SIMULINK software.

ACKNOWLEDGEMENT

"This work was supported primarily by the ERC program of the National Science Foundation under Award Number EEC-9731677."

REFERENCES

[1] D. G. Holmes, and A. Kotsopoulos, "Variable speed control of single and two phase induction motors using a three phase voltage source inverter," in *IEEE/IAS Annual Meeting Conference Record*, October 1993, pp. 613-620,.

[2] E.R. Collins Jr, H. B. Püttgen, and I. W. E. Sayle, "Single-phase induction motor adjustable speed drive: Direct phase angle control of the auxiliary winding supply," in *IEEE/IAS Annual Meeting Conference Record*, IEEE, IAS-88, October 1992, pp. 246-252.

[3] E.R. Collins Jr,, "Torque and slip behavior of single-phase induction motors driven from variable speed supplies," in IEEE, IAS-90, pp. 246-252.

[4] E.R. Collins Jr, R. E. Ashley, "Operating characteristics of single-phase capacitor motors driven from variable speed supplies," in IEEE, IAS-91, pp. 52-57.

[5] T. A. Lipo, "Motor / Converter topologies for low cost HVAC Application," short report, 1999.

[6] F. E. Wills, H. R. Schnetzka, and R. D. Hoffer, "US Patent 5146147, AC motor drive system," 1992.

[7] F. E. Wills, H. R. Schnetzka, and R. D. Hoffer, "US Patent 5136216, AC motor drive system," 1992.

[8] F. E. Wills, H. R. Schnetzka, and R. D. Hoffer, "US Patent 5218283, AC motor drive system with a two phase power supply," 1993.

[9] P. C. Krause, "Simulation of Unsymmetrical 2-Phase Induction Machines," *IEEE Transactions on Power Apparatus and Systems*, vol. PAS-84, NO. 11, 1965, pp. 1025-1037.

[10] A. M. Trzynadlowski, F. Blaabjerge, J.K. Pederson, L. Kirlin, S. Logowski, "Random pulse width modulation technique for converter-fed drive systems – A review," in *IEEE Trans. On Industry Application*, vol. 30., no. 5, 1994, pp. 1166-1174.

[11] J. Mahdavi, Sh. Kaboli, and H.A. Toliyat, "Conducted electromagnetic emissions in unity power factor ac/dc converters: comparison between PWM and RPWM techniques," *in IEEE, PESC 99*, pp. 881-885

[12] E.R. Benedict, T.A. Lipo, "Improved PWM modulation for a permanent-split capacitor motor," *in IEEE, IAS, 2000*.

[13] M. A. Boost, and P. D .Ziogas, , "State-of-the-Art Carrier PWM Techniques: A Critical Evaluation," *IEEE Transactions on Industry Applications*, vol. 24, 1998, pp. 271-280.

[14] Van der Broeck H., "Circuit arrangement for powering a two phase asynchronous motor," "US Patent 5,446,361, August, 1995.